Modeling and Characterization of Lathe Spindle Cutting Patterns with Crossed Roller Bearing Installed

Xiaozhong Song, Xianghua Zhou, Rahul Chaudhari, Stephen P. Johnson, and Mike Kotzalas
The Timken Company, North Canton, Ohio 44720, USA
Email: xiaozhong.song@timken.com, {andy.zhou, rahul.chaudhari, stephen.johnson, machiel.kotzalas}@timken.com

Abstract—**The cutting pattern is the primary surface profile remaining on a lathe-turned surface along the tool feed direction. It reflects the cutting depth variation of each feed step distance. Cutting pattern evaluation is an important part of the spindle inspection process for a newly built lathe machine and is widely used by machine tool builders. Yet, how the pattern is generated and affected by the bearing has not been clearly understood prior to the presentation of this study. Pattern evaluation currently is completed by running a cut test under designed cutting parameters and visual checking by experienced quality control personnel. But because these patterns are not clearly understood, their qualification and quantification become a challenge for the machine builders and bearing maker. In this paper, a bearing spindle cutting pattern model has been developed and presented for the characterization of crossed roller bearings in a lathe machine spindle, which clearly indicated how the pattern comes from and it could be quantified for evaluation comparison. The underlying theory was derived from the relationship of turning motion in part rotation and cutting tool feed in a straight line along the axial direction. The modeling algorithm uses spindle run out FFT to get the spindle bearing feature frequency's motion in the circumference direction, which is then synchronized at each cutting spot along the feed direction to modulate the tool and work piece pattern track. The model has been validated by simulated bearing feature frequencies and benchmark machine tests. The model's characterized pattern was found to match closely with the actual cut pattern.**

Index Terms—**crossed roller bearing, lathe spindle bearing, spindle runout, cutting pattern, FFT analysis, modulation**

I. Introduction and Problem Identification

Crossed roller bearings are designed to offer the highest levels of rotational accuracy and rigidity while conserving space and saving material costs. These bearings feature two sets of races and rollers brought together at right angles, with alternate rollers facing in the opposite direction and fit into two race spaces. Each roller held apart by separators that perform a "cage" function to keep the roller in position and reduce the friction caused by the rollers contacting each other. Their advantageous characteristics have resulted in crossed roller bearings becoming widely used in the machine tool building industry as large table lathe machines' main spindle support bearings.

Crossed roller bearings are often delivered as separate parts and require installation at user sites. In addition to the bearing components' manufacturing accuracy, the bearing's cutting performance is also affected by whether it is installed properly. When machine builders install bearings, they follow the manufacturer's installation guidelines to correctly install the bearing. After installation, the machine must go through real cutting tests to ensure the spindle bearing system can meet the cutting criteria. The machined surface roughness (mainly affected by tool geometry, feed rate and vibration) and cutting pattern (it reflected cutting depth variation in each feed step distance) are the parameters usually evaluated. Currently the first item, surface R_{max}, is used to quantify the evaluation. The second item, cutting pattern, is evaluated by experienced quality personnel and should be visually smooth and even.

After the test cut, occasionally the machined surface roughness and cutting patterns cannot pass the evaluation because they exhibit chatter-like cutting and high surface roughness, even after adjusting the cutting parameters. Fig. 1 shows this symptom from one test on a newly built lathe in which a crossed roller bearing was installed. In this situation, usually the machine builder will reinstall the bearing and try again. Sometimes the second try results in acceptable performance, but generally it doesn't, and a new bearing must be installed and another test performed until acceptable results are produced. Since the builder doesn't know what will cause of chatter like cutting and high roughness and consequently doesn't know how to efficiently correct it, this kind tries out not only waste labor, but also affect machine delivery time. Most important, it is likely that this chatter-like pattern is not actual spindle bearing system chatter vibration — yet the bearing is still treated as if it were the cause of the quality problem and is rejected, causing an increase in the customer's and bearing manufacturer's business costs from shipping the bearings back and forth.

This problem has existed in the crossed roller bearing market for some time, but there has been no published literature showing that any research has been done to identify the root cause of these unacceptable cutting patterns until the authors' recent investigation. Aside

Manuscript submission July 26, 2018; accepted July 7, 2019.

doi: 10.18178/ijmerr.8.5.660-666

from situations where the bearing's roller and rings are actually defective, the cutting pattern also has been found to arise from the bearing rollers' "gap" not being adjusted properly, which creates uneven rolling motion in the rollers' train and finally modulates a low-frequency chatter-like motion of the spindle that synchronizes in the cutting feed direction and forms a vibration-like cutting pattern, as shown in Fig. 1. Further analysis shows this pattern also affects the surface roughness value R_{max}.

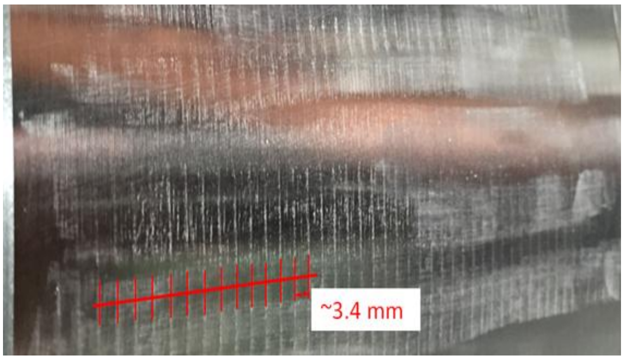

Figure 1. Unacceptable chatter-like cutting pattern on the turned surface (Cutting speed 200m/min, DOC 0.2 mm and feed 0.143 mm/rev, aluminum material)

There are many published technical articles about machine spindle performance in which several researchers have studied spindle error motion as related to rolling elements and hydrostatic bearing performance. S. Noguchi et al. developed a bearing radial runout measurement method that could test a bearing's non-repeatable form error when in load condition. Their findings show that bearing cage and ball size variation has much more effect than rings in spindle runout performance [1], [2]. Zhaohui Yang, Jun Hong, et al. developed a double sensor spindle error motion measurement method and algorithm to separate the radial runout signal from noise to determine the spindle's running form error [3]. Ramesh H. Aralaguppi et al. investigated how CNC machine spindle thermal tilt affected bore machining accuracy [4]. Further, a spindle error motion analyzer called the SAE System was developed by Lion Precision Company in cooperation with Dr. Eric R. Marsh from Pennsylvania State University. It can accurately perform spindle bearing error motion measurements and quantity analysis, and based on the results can characterize spindle running performance by synchronous and asynchronous error motion value [5]. However, none of the chatter-like cutting pattern issues have been explored in any of those studies, even though this topic has very great significance for machine builders.

In order to complement current bearing production and performance diagnostic practices, in this paper a modeling method has been developed and presented for the characterization of chatter-like cutting patterns for a crossed roller bearing-installed lathe machine spindle. This method solved where it comes from and could be used for spindle cutting performance quantitation evaluation and narrow down the root cause diagnostics of unacceptable patterns. The modeling includes:

(1) Using an LVDT displacement sensor to directly measure the spindle (where a crossed roller bearing has been installed to support it) radial runout in a relatively long rotation period and collect the runout data;
(2) Performing the FFT analyses on the runout data to determine the possible spindle bearing defect frequencies and their amplitude;
(3) Based on the found frequency components, building a spindle runout model in the time domain;
(4) Estimating the cutting pattern by running the synchronized modulating algorithm on the spindle per revolution timing;
(5) Running the cutting feed direction data processing with the spindle synchronized modulating algorithm on the real runout data. The results are the instant spindle motion in cutting feed direction at cutting point. This can be used to validate the modeling accuracy.

II. Bearing Defective Frequency and Spindle Cutting Pattern Performance Modeling

A. Bearing Defective Frequency

Fig. 2 illustrates a general, simplified model of a rolling element bearing. In this model, the bearing will exhibit characteristic frequencies when it is in defective status.

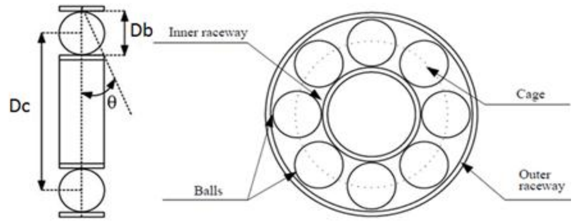

Figure 2. General model of rolling element bearing

Under most conditions, the four most important characteristic defective frequencies are fundamental cage frequency FC, ball pass inner raceway frequency FBPI, ball pass outer raceway frequency FBPO, and ball pin frequency FB. These characteristic frequencies can be modeled by the following equations [6]. These frequency components appear in the frequency spectrum when the bearings are in defective status, either from manufacturing defects or when their components are subject to tensions and deformations caused by improper installation.

$$F_C = \frac{1}{2} F_S \left(1 - \frac{D_b \cos(\theta)}{D_c} \right). \tag{1}$$

$$F_{BPI} = \frac{N_B}{2} F_S \left(1 + \frac{D_b \cos(\theta)}{D_c} \right). \tag{2}$$

$$F_{BPO} = \frac{N_B}{2} F_S \left(1 - \frac{D_b \cos(\theta)}{D_c}\right). \tag{3}$$

$$F_B = \frac{D_c}{2D_b} F_S \left(1 - \frac{D_b^2 \cos^2(\theta)}{D_c^2}\right). \tag{4}$$

where: D_b is the ball diameter; θ is the contact angle based on the ratio of axial to radial load; D_c is the cage diameter; N_B is the number of balls; F_S is the shaft rotational frequency.

Close examination of these defective frequencies finds that no matter what the contact angle θ is, these frequencies are not all harmonics with spindle rotation frequency F_S. The fundamental cage frequency F_C is always lower than the shaft-spindle rotation frequency, and the other three frequencies F_{BPI}, F_{BPO} and F_B are always higher. These characteristics are very important when the details of the bearing parameters are unknown but the spindle defective spectrum still can be measured and estimated. Using this rule, which part of the bearing the bearing defects are from still can be identified.

Next, in the cutting pattern modeling section of this paper, we will see that these four frequencies are the main contributors to the cutting pattern — and whenever these non-spindle rotation runout harmonics exist, the cutting patterns are always modulated to the cutting feed direction.

B. *Cutting Pattern Modeling from Bearing Defective Frequency*

Fig. 3 shows a general cutting motion relationship when a straight profile is cut on a lathe machine, where the work is creating the rotation motion and the tool just moves in a straight line along the axial direction.

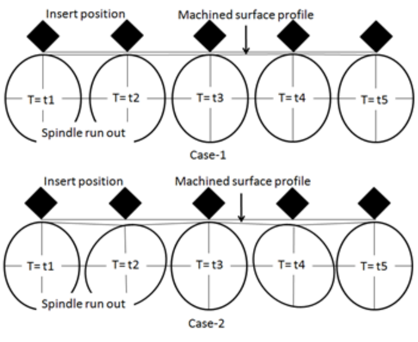

Figure 3. Cutting pattern formation model

where: T = t_1, t_2, t_3 … represent the cutting tool feed time in the spindle rotated in one complete circle interval

In the illustration it can be seen that in Case 1, even the spindle has radial runout (oval shape), but its orientation is synchronized with the spindle rotation RPM and the tool feed rate pace. So, when the insert moves to the cutting points (t_1, t_2, t_3 …), the cutting pattern exhibits the same depths that formed on the machined surface profile along the axis in a straight line, and leaves only insert tip radius shapes on the surface (which is the cutting contribution of surface roughness). In Case 2, since the spindle bearing runout is not synchronized with spindle RPM, at each cutting point t_1, t_2, and t_3 … the cutting process removes different depths of stock at different spots. Except for surface roughness, the surface profile generated under this condition demonstrates an additional cutting pattern that sometimes looks like chatter marks.

In an actual lathe spindle with rolling element bearings installed, the radial motion or runout at the cutting point is much more complicated than in the above illustration and will look more like Fig. 4. It could contain all the bearing basic characteristic frequencies indicated by Equations (1)–(4) and their harmonic components.

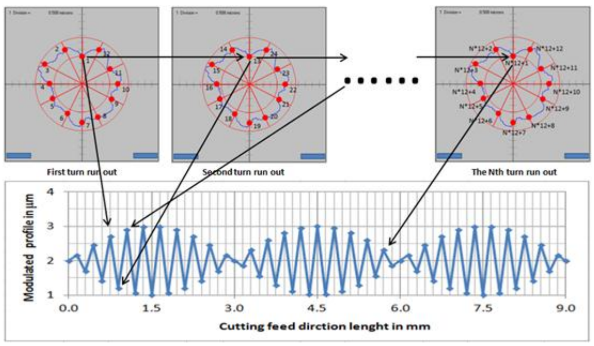

Figure 4. Model cutting pattern identification

Fig. 5 illustrates an actual cut surface profile with significant cutting patterns on it. In the plot shown, the red line represents the cutting pattern, which is the relative motion between part surface and tool position at the cutting points. In the overall profile, it also can be observed that the surface roughness R_{max} is the combination of the cutting pattern amplitude plus tool nose-formed surface periodic peaks.

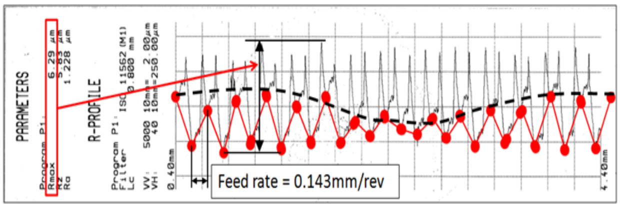

Figure 5. Actual cut profile and its cutting pattern identification

The bearing spindle runout that contributes to the generation of real cutting patterns can be represented by the following equation

$$\begin{aligned} Y(t) = {} & A_1\mathrm{Sin}(2\pi F_S)t + A_2\mathrm{Sin}(2\pi F_C)t + A_3\mathrm{Sin}(2\pi F_{BPI})t \\ & + A_4\mathrm{Sin}(2\pi F_{BPO})t + A_5\mathrm{Sin}(2\pi F_B)t + A_6\mathrm{Sin}(2{*}2\pi F_S)t \\ & + A_7\mathrm{Sin}(2{*}2\pi F_C)t + A_8\mathrm{Sin}(2{*}2\pi F_{BPI})t + A_9\mathrm{Sin}(2{*}2\pi F_{BPO})t \\ & + A_{10}\mathrm{Sin}(2{*}2\pi F_B)t + \ldots + A_{N+1}\mathrm{Sin}(N{*}2\pi F_S)t \\ & + A_{N+2}\mathrm{Sin}(N{*}2\pi F_C)t + A_{N+3}\mathrm{Sin}(N{*}2\pi F_{BPI})t \\ & + A_{N+4}\mathrm{Sin}(N{*}2\pi F_{BPO})t + A_{N+5}\mathrm{Sin}(N{*}2\pi F_B)t \end{aligned} \tag{5}$$

where: A_1, A_2, A_3 … A_{N+5} are runout amplitudes at the bearing characteristic frequencies.

In actual cutting applications, at the time of each revolution cutting point, $t = n/Fs$, $n = 0, 1, 2 \ldots N$ (along the cutting feed direction). At these points, the spindle runs out:

$$\begin{aligned} Y(n/Fs) &= A_1 Sin(2\pi Fs)(n/Fs) + A_2 Sin(2\pi Fc)(n/Fs) + \\ & A_3 Sin(2\pi F_{BPI})(n/Fs) + A_4 Sin(2\pi F_{BPO})(n/Fs) + \\ & A_5 Sin(2\pi F_B)(n/Fs) + A_6 Sin(2*2\pi Fs)(n/Fs) \\ & + A_7 Sin(2*2\pi Fc)(n/Fs) + A_8 Sin(2*2\pi F_{BPI})(n/Fs) \\ & + A_9 Sin(2*2\pi F_{BPO})(n/Fs) + A_{10} Sin(2*2\pi F_B)(n/Fs) + \ldots + \\ & A_{N+1} Sin(N*2\pi Fs)(n/Fs) + A_{N+2} Sin(N*2\pi Fc)(n/Fs) + \\ & A_{N+3} Sin(N*2\pi F_{BPI})(n/Fs) + A_{N+4} Sin(N*2\pi F_{BPO})(n/Fs) + \\ & A_{N+5} Sin(N*2\pi F_B)(n/Fs) \end{aligned}$$

$$\begin{aligned} &= A_1 Sin(2n\pi) + A_2 Sin(2n\pi Fc/Fs) + A_3 Sin(2n\pi F_{BPI}/Fs) \\ & + A_4 Sin(2n\pi F_{BPO}/Fs) + A_5 Sin(2n\pi F_B/Fs) + \\ & A_6 Sin(2*2n\pi Fs/Fs) + A_7 Sin(2*2n\pi Fc/Fs) + \\ & A_8 Sin(2*2n\pi F_{BPI}/Fs) + A_9 Sin(2*2n\pi F_{BPO}/Fs) + \\ & A_{10} Sin(2*2n\pi F_B/Fs) + \ldots + A_{N+1} Sin(N*2n\pi Fs/Fs) \\ & + A_{N+2} Sin(N*2n\pi Fc/Fs) + A_{N+3} Sin(N*2n\pi F_{BPI}/Fs) \\ & + A_{N+4} Sin(N*2n\pi F_{BPO}/Fs) + A_{N+5} Sin(N*2n\pi F_B/Fs) \\ &= 0 + A_2 Sin(2n\pi Fc/Fs) + A_3 Sin(2n\pi F_{BPI}/Fs) \\ & + A_4 Sin(2n\pi F_{BPO}/Fs) + A_5 Sin(2n\pi F_B/Fs) + \\ & A_6 Sin(2*2n\pi Fs/Fs) + A_7 Sin(2*2n\pi Fc/Fs) + \\ & A_8 Sin(2*2n\pi F_{BPI}/Fs) + A_9 Sin(2*2n\pi F_{BPO}/Fs) + \\ & A_{10} Sin(2*2n\pi F_B/Fs) + \ldots + A_{N+1} Sin(N*2n\pi Fs/Fs) \\ & + A_{N+2} Sin(N*2n\pi Fc/Fs) + A_{N+3} Sin(N*2n\pi F_{BPI}/Fs) \\ & + A_{N+4} Sin(N*2n\pi F_{BPO}/Fs) + A_{N+5} Sin(N*2n\pi F_B/Fs) \end{aligned} \quad (6)$$

Equation (6) is the final spindle cutting pattern model along the axial direction with the revolution number n as the variable. It is the accurate model for a gage profile along the cutting direction

From the engineering practice point of view, the higher harmonic components are rather small. The main contributions to the cutting pattern are from the first-order frequency components, so the model of the cutting pattern could be simplified as:

$$\begin{aligned} Y(n/Fs) &= A_1 * 0 + A_2 Sin(2n\pi Fc/Fs) + A_3 Sin(2n\pi F_{BPI}/Fs) \\ & + A_4 Sin(2n\pi F_{BPO}/Fs) + A_5 Sin(2n\pi F_B/Fs)) \end{aligned} \quad (7)$$

where: $n = 1, 2, 3 \ldots N$ is the integer of the spindle turned revolution number

In the model, the bearing characteristic frequencies can be derived directly from the bearing dimensions. The algorithm for the detail modeling of the spindle cutting pattern was developed using Excel functions. The procedure is outlined in Fig. 6.

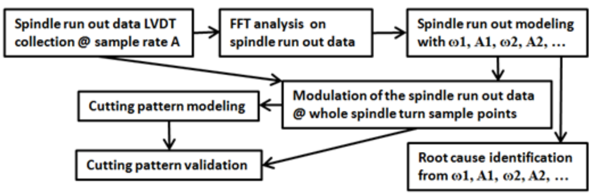

Figure 6. Modeling algorithm for cutting pattern

C. Simulation of the Cutting Pattern Modeling

To assess the model's accuracy, one specific crossed roller bearing has been scrutinized. It's bearing defective frequencies (1) (2) (3) and (4) are calculated in Table 1. Fig. 7 shows the simulation results using a defect frequency that matches with just one of the bearing fundamental frequencies and predicts the cutting feed direction toolpath modulation pattern.

TABLE I. TEST CROSSED ROLLER GEOMETRY AND FEATURE FREQUENCIES

Contact α	42.95	Pitch Dia	537.816	Roller Dia	30.759	Roller #	21	Spndl RPM	5
Feature frequency	Basic	2 harmonic	3 harmonic	4 harmonic	5 harmonic	6 harmonic	7 harmonic	8 harmonic	9 harmonic
F_S (Hz)	0.083	0.167	0.250	0.333	0.417	0.500	0.583	0.667	0.750
F_B (Hz)	0.727	1.454	2.182	2.909	3.636	4.363	5.091	5.818	6.545
F_{BPO} (Hz)	0.838	1.677	2.515	3.353	4.192	5.030	5.869	6.707	7.545
F_{BPI} (Hz)	0.912	1.823	2.735	3.647	4.558	5.470	6.381	7.293	8.205
F_C (Hz)	0.043	0.087	0.130	0.174	0.217	0.260	0.304	0.347	0.391

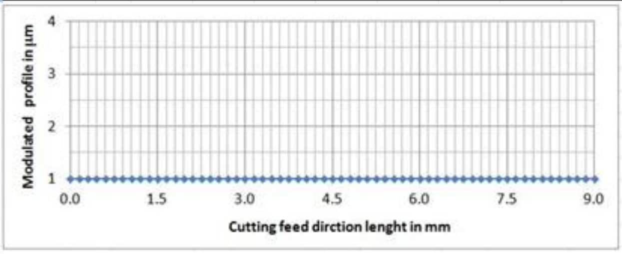

Case 1. All the defective frequencies' amplitude = 0, cutting pattern is a straight line

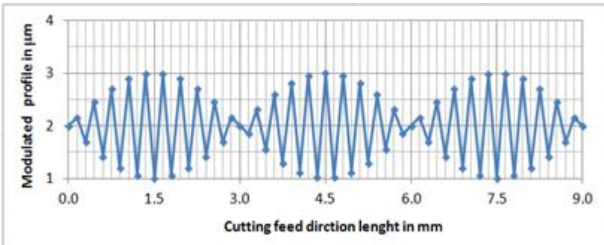

Case 2. Only defective frequency is F_C and its amplitude = 2 um, cutting pattern is chatter-like vibration line

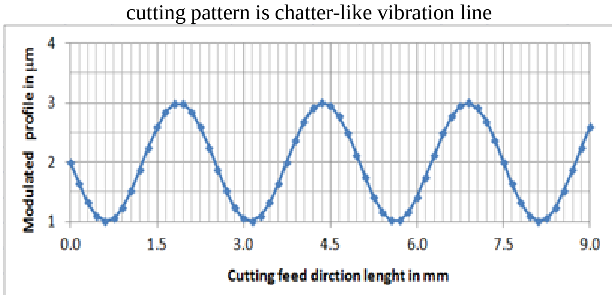

Case 3. Only defective frequency is F_{BPI} and its amplitude = 2 um, Cutting pattern is a low-frequency sine type wave line

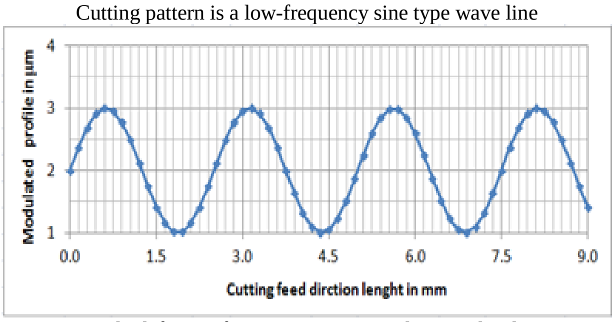

Case 4. Only defective frequency is F_{BPO} and its amplitude = 2 um Cutting pattern is a low-frequency sine type wave line

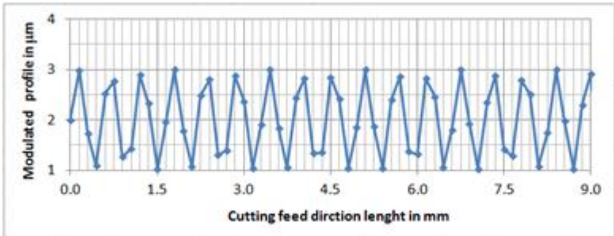

Case 5. Only defective frequency is F_B and its amplitude = 2 um, cutting pattern is a middle frequency sine wave line

Figure 7. Cutting pattern simulation results

The results in the above model show that all the defect frequencies modulate a cutting pattern, but different defect frequency components modulate different patterns. In simulation, the model uses equal defect frequency amplitudes to simulate the cutting pattern. But in a real machine spindle bearing system, since they are all mechanical vibrations, as the characteristic frequencies increase, the amplitude of the vibration response will reduce — so the amplitude at higher frequencies will be much smaller than those in the low-frequency zone. As mentioned above, the lowest defect frequency of all the possible four defect frequencies is F_C. If the variation of cutting depth with tool feed is compared, the chatter-like motion appears only when F_C exists. The other patterns do not resemble the chatter pattern and normally their amplitudes are much smaller than the F_C modulated pattern. In most applications observed by the authors, all the defect frequencies were present, but only one or two of them were significant in their excitation of a modulated cutting pattern response.

III. Machine Spindle Bearing System Cutting Pattern Characterization

A. Setup and Sample Rate Selection

The test objective was to validate the model with a real machine spindle bearing system's runout data. In the test, the linear variable differential transformer (LVDT) displacement sensor was used as the main spindle runout data collection unit. The LVDT sensor can capture runout data at sub-micron accuracy and has good low-frequency response up to ~20 Hz. By comparison, the most commonly used vibration sensors (e.g., velocity and acceleration sensors), have a frequency response that starts around 10 Hz with the added disadvantage that they can't directly measure the displacement. According to the pre-trial tests, the spindle RPM setup range of 6~60 appears reasonable. Fig. 8 shows the spindle runout data collection setup at one machine builder's testing site.

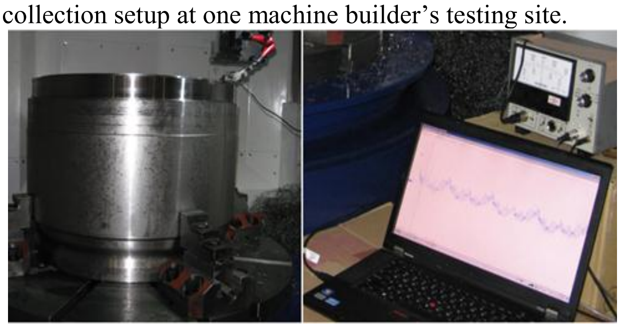

Figure 8. LVDT spindle runout measurement setup

In theory, the model uses the synchronization data method to process the data pattern modulation. The measurement data is not particularly sensitive to surface quality, but in order to minimize any kind of possible measurement noise, the measurement surface must be pre-cut on the machine to correct work off-center mounting error and uneven black surface stock distribution. The LVDT sensor head was mounted at the machine tool holder position, and the sensor tip was located as close as possible to the same spot as the cutting tool/workpiece contact point.

The data acquisition sample rate was set at a range of 20 Hz~120 Hz. When the lower sample rate of 20 Hz is selected and a spindle speed of 6 RPM is selected, the result is 360°/200 points = 1.8°/point. When a higher RPM is selected, the sample rate can be increased to keep the similar sampling resolution. As mentioned before, the cutting pattern modulation exhibited a long wavelength and hence data should be recorded for 40-60 full revolutions of the work spindle.

B. Benchmark Machine Spindle Runout and Cutting Pattern Modulation

A lathe with a precision hydrostatic spindle was selected as the benchmark machine to run the tests and collect the data from the model's spindle bearing cutting pattern performance evaluation. Its spindle bearing runout specification is less than 0.15 μm. The test was conducted by center chucking one cylinder steel bar (diameter 50 mm x length 85 mm) in the lathe, then using a speed of 160m/min, feed 0.1mm/rev and DOC 0.1mm to straight cut the body surface. After cutting, keeping the bar in the chuck centers, the radial direction runout was measured with the LVDT toward the spindle side. The experimental spindle radial runout is shown in Fig. 9 (a) in the time domain. Fig. 9 (b) is its FFT analysis result in the frequency domain. Its cutting pattern modeling analysis result is shown in Fig. 9 (c). Where the runout measurement sample rate was set at 60 points/second, the spindle RPM was 30, so the number of sample points per revolution equaled 120. The FFT analysis data show that all the spindle runout amplitudes at each frequency were less than 0.4μm and were harmonics of the shaft running frequency. All the amplitudes of the characteristic frequencies (1) (2) (3) (4) were zero (none of those frequencies show up on the FFT chart). These parameters were put in the model (Equation (7)). All the parameters in the model were near zero, which means the cutting pattern is a straight line. The cutting pattern modeling analysis data showed that the hydrostatic bearing had very good cutting pattern performance. The chatter-like cutting pattern contribution from the spindle bearing runout modulation was zero, and the total contribution to the cutting pattern was less than 0.2 μm — almost a straight-line profile, as shown in Fig. 9 (c).

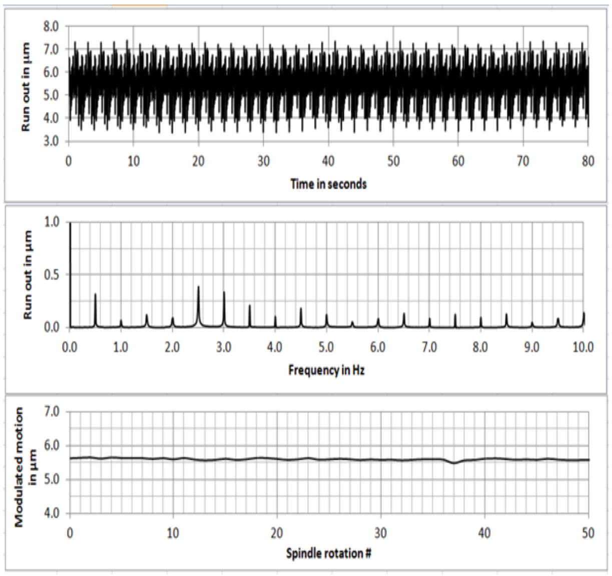

Figure 9. (a), (b), (c). High-precision hydrostatic spindle bearing's cutting pattern evaluation

C. Lathe Spindle Bearing with Chatter-like Cutting Pattern

The cutting pattern of the second test lathe was known to demonstrate chatter-like behavior. The test setup is shown in Fig. 8. Its radial runout data is shown in Fig. 10 (a) in the time domain. Fig. 10 (b) is the FFT analysis result in the frequency domain, and its cutting pattern modeling analysis result appears in Fig. 10 (c). Where the runout measurement sample rate was set at 40 points/second, the spindle RPM was 5, so one complete spindle revolution equaled 480 points. The cutting pattern modeling analysis demonstrated that this machine's spindle bearing performed poorly because its modulated cutting pattern contribution from spindle bearing performance was about 5~6μm and chatter-like patterns in groups along the cutting feed direction were clearly observed, as seen in Fig. 10 (c). This lathe was built with a crossed roller bearing as the main spindle support. Its pattern looks the same as the one the machine builder visually found on the test cut surface profile when the test cut was run.

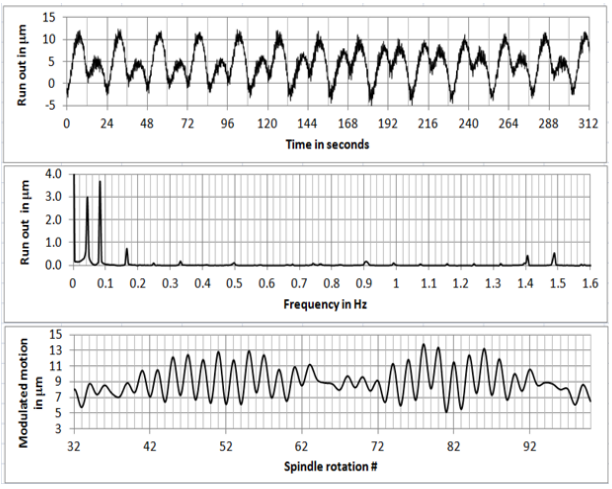

Figure 10. (a), (b), (c). Incorrectly installed crossed roller bearing spindle cutting pattern evaluation

D. Results, Discussion and Root Cause Validation

Comparison of these two lathe tests reveals that the second machine developed significant chatter-like cutting pattern in its profile. The first benchmark machine has hardly any significant fluctuation in its surface profile. Further examination of the first machine's spindle FFT spectra indicates that because a hydrostatic bearing was used, there is no cage inside the bearing, and the lowest frequency shown on the spectrum chart is 0.5 Hz, which is the spindle rotation frequency (30 RPM/60 minutes = 0.5Hz). All the other frequencies have a harmonic relationship with the spindle rotation frequency. This means that although the spindle has many runout components, since they are always synchronous with the spindle rotation frequency they will not be modulated to the cutting direction — so no cutting pattern was influenced by them.

In the second machine, it can clearly be seen that there is a high amplitude value at the fundamental cage frequency component F_C (at the 0.0426 Hz position). It has been identified by bearing defect frequency Equation (1) using the bearing design parameters. Alternatively, the rule mentioned above could be used, wherein of all the defective frequencies, only the fundamental cage frequency F_C is lower than the spindle rotation frequency, which in this case was 5 RPM/60 minutes = 0.0833 Hz. Except for these two significant runout frequencies, there were no other significant frequencies. A look at the related modulated profile reveals that the second machine has a very significant chatter-like motion pattern on the surface along the cutting feed direction. With these comparisons, it can now be concluded that the chatter-like cutting pattern from a crossed roller bearing spindle is caused by the presence of a fundamental cage defect frequency of some minimum amplitude. Furthermore it was observed that the amplitude of the cage defective frequency F_C correlated with roller separator setting established during bearing installation. Fig. 11 shows after adjusting the setting of the roller separators that make up the cage in the crossed roller bearing, the fundamental cage frequency component F_C dropped to a very low level (less than 1μm), and following this adjustment the chatter-like cutting pattern almost completely disappeared.

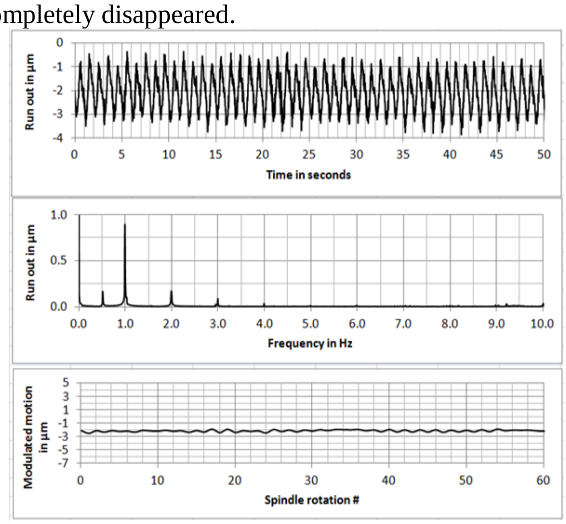

Figure 11. (a), (b), (c). Correctly installed crossed roller bearing spindle cutting pattern where roller separators have been adjusted

IV. Conclusions

Based on the investigation and real case tests, the following conclusions can be drawn:

a) A lathe spindle cutting pattern model was developed using two lathe machines with different bearing types installed. Results from actual test cuts compared well with modeling predictions.

b) The spindle cutting pattern was identified and characterized quantitatively through modeling. Different bearing defect frequencies were shown to modulate different cutting patterns. The correlation between cutting pattern and defect frequency could be used diagnostically to determine root cause when the unacceptable cutting pattern was observed in the testing

c) It was demonstrated that the pattern of most concern for machine builders — the chatter-like cutting pattern, is due to the presence of a fundamental cage frequency response in the bearing. Comparing results from two test cases, a hydrostatic bearing equipped spindle versus a cross roller bearing equipped spindle. A correlation between the setup of the roller separators and the amplitude of fundamental cage frequency vibration on the cross roller bearing was observed.

d) Modeling and testing demonstrated that minimizing the amplitude of the fundamental cage frequency vibration is critical to achieving acceptable on-machine cutting patterns.

References

[1] S. Noguchi, B. Noda, and K. Sasajima, "The Influence of location of balls and ball diameter difference in rolling bearings on the non-repetitive runout (NRRO) of retainer revolution," *Precision Engineering*, vol. 29, pp. 11–18, 2005.

[2] S. Noguchi and T. Kanada, "Development of measuring system for radial Non-Repetitive Run-Out (NRRO) and perception about present state of angular contact ball bearing for machine tools," *Tribology International*, vol. 41, no. 12, pp. 1176–1180, 2008.

[3] Z. H. Yang, J. Hong, J. H. Zhang, M. Y. Wang, "Research on the rotational accuracy measurement of an aerostatic spindle in a rolling bearing performance analysis instrument," *International Journal of Precision Engineering and Manufacturing*, vol. 15, no. 7, pp. 1293–1302, July 2014

[4] R. H. Aralaguppi, T. Subramanian, "Study of spindle rotational accuracy versus bore accuracies on the machined test piece on the CNC machining centre," *iNacoMM 2015-213*, Kanpur, India, Dec 16–19, 2015

[5] E. R. Marsh, "Precision spindle metrology," DES Tech Publications, 2008

[6] E. Mendel, T. W. Rauber, F. M. Varejão, and R. J. Batista, "Rolling element bearing fault diagnosis in rotating machines of oil extraction rigs," *17th European Signal Processing Conference (EUSIPCO 2009)*, Glasgow, Scotland, August 24–28,